BIOCHEMISTRY
including biophysical chemistry & molecular biology
Article

Biochemistry **2009,** *48,* 6909–6920 6909
DOI: 10.1021/bi900854z

Targeting and Insertion of the Cholesterol-Binding Translocator Protein into the Outer Mitochondrial Membrane†

Malena B. Rone,[‡,§] Jun Liu,[‡] Josip Blonder,[@] Xiaoying Ye,[@] Timothy D. Veenstra,[@] Jason C. Young,[∥] and Vassilios Papadopoulos*[,‡,§,∥,⊥]

[‡]*Department of Biochemistry, Molecular and Cellular Biology, Georgetown University Medical Center, Washington, D.C. 20007,* [§]*The Research Institute of the McGill University Health Centre and Department of Medicine and* [∥]*Department of Biochemistry and* [⊥]*Department of Pharmacology and Therapeutics, McGill University, 1650 Cedar Avenue, Montreal, Quebec H3G 1A4, Canada, and* [@]*Laboratory of Proteomics and Analytical Technologies, SAIC-Frederick Inc., National Cancer Institute at Frederick, Frederick, Maryland 21702*

Received May 20, 2009; Revised Manuscript Received June 23, 2009

ABSTRACT: Translocator protein (18 kDa, TSPO), previously known as the peripheral-type benzodiazepine receptor, is an outer mitochondrial membrane (OMM) protein necessary for cholesterol import and steroid production. We reconstituted the mitochondrial targeting and insertion of TSPO into the OMM to analyze the signals and mechanisms required for this process. Initial studies indicated the formation of a mitochondrial 66 kDa complex through Blue Native-PAGE analysis. The formation of this complex was found to be dependent on the presence of ATP and the cytosolic chaperone Hsp90. Through mutational analysis we identified two areas necessary for TSPO targeting, import, and function: amino acids 103−108 (Schellman motif), which provide the necessary structural orientation for import, and the cholesterol-binding C-terminus required for insertion. Although the translocase of the outer mitochondrial membrane (TOM) complex proteins Tom22 and Tom40 were present in the OMM, the TOM complex did not interact with TSPO. In search of proteins involved in TSPO import, we analyzed complexes known to interact with TSPO by mass spectrometry. Formation of the 66 kDa complex was found to be dependent on an identified protein, Metaxin 1, for formation and TSPO import. The level of import of TSPO into steroidogenic cell mitochondria was increased following treatment of the cells with cAMP. These findings suggest that the initial targeting of TSPO to mitochondria is dependent upon the presence of cytosolic chaperones interacting with the import receptor Tom70. The C-terminus plays an important role in targeting TSPO to mitochondria, whereas its import into the OMM is dependent upon the presence of the Schellman motif. Final integration of TSPO into the OMM occurs via its interaction with Metaxin 1. Import of TSPO into steroidogenic cell mitochondria is regulated by cAMP.

Translocator protein (18 kDa, TSPO),[1] previously known as the peripheral-type benzodiazepine receptor, is an 18 kDa, high affinity, cholesterol- and drug-binding protein that is located in the outer mitochondrial membrane (OMM). TSPO appears to contain five α-helices that span the OMM and assist with the transport of cholesterol from intracellular stores to the mitochondrial matrix, the rate-limiting step in steroid biosynthesis (*1*−*3*). TSPO has been shown to interact with the voltage-dependent anion channel (VDAC) and the adenine nucleotide transporter (ANT) comprising the mitochondria permeability transition pore (MPTP), which is located at the contact site between the inner and outer mitochondrial membrane (*4*−*8*). This mitochondrial localization at the contact site influences many of the biological functions in which TSPO participates, including cholesterol transport, protein import, cell proliferation, and apoptosis (*1*, *2*, *9*−*15*). Because of its key role in these cellular functions, the targeting and insertion of TSPO into the OMM are thought to be tightly regulated.

Like the majority of mitochondrial proteins, TSPO is genetically encoded in the nucleus, translated in the cytosol, and then imported into mitochondria (*16*−*18*). Unlike many mitochondrial

†This work was supported by National Institutes of Health Grant ES07747 and in part by Grant HD37031 (to V.P.). V.P. was also supported by a Canada Research Chair in Biochemical Pharmacology. J.C.Y. holds a Canada Research Chair in Molecular Chaperones. The Research Institute of MUHC is supported by a Center grant from Le Fonds de la recherche en santé du Québec.

*To whom correspondence should be addressed: The Research Institute of the McGill University Health Centre, 1650 Cedar Ave., C10-148, Montreal, Quebec H3G 1A4, Canada. Telephone: (514) 934-1934, ext. 44580. Fax: (514) 934-8439. E-mail: vassilios.papadopoulos@mcgill.ca.

[1]Abbreviations: ANT, anion nucleotide transporter; BN-PAGE, Blue Native polyacrylamide gel electrophoresis; FBS, fetal bovine serum; GD, geldanamycin; Hsp, heat shock protein; IMM, inner mitochondrial membrane; MPTP, mitochondria permeability transition pore; NB, novobiocin; OMM, outer mitochondrial membrane; SDS−PAGE, sodium dodecyl sulfate−polyacrylamide gel electrophoresis; StAR, steroidogenesis acute regulatory protein; TOM, translocase of the outer mitochondrial membrane; TSPO, translocator protein (18 kDa); VDAC, voltage-dependent anion channel; SAM, sorting and assembly machinery.

Published on Web 06/24/2009

proteins of the matrix and inner mitochondrial membrane, OMM proteins such as TSPO do not have cleavable presequences for mitochondrial targeting. Instead, these proteins are targeted to the OMM through internal amino acid sequences (*19*). To date, OMM targeting signals have not been defined or predicted in multimembrane spanning proteins, and the signal or signals within TSPO are unknown.

The translocase of the outer mitochondrial membrane (TOM) complex is a protein complex composed of receptors that recognize mitochondrial proteins for import and an aqueous pore for the translocation of proteins across the membrane (*20*). The TOM complex includes the key components Tom22 and Tom40, the latter of which forms the translocation pore (*21*). Additional import complexes further direct the protein to its correct location in the OMM, inner mitochondrial membrane (IMM), intermembrane space, and mitochondrial matrix. The TOM receptor protein, Tom70, has been shown to loosely associate with the TOM complex and is important for the import of IMM metabolite carriers that have internal targeting sequences as well as larger hydrophobic proteins (*22*). Tom70 functions as a docking protein for both Hsc70 and Hsp90 through a central tetratriacopeptide repeat domain (*23*), while its C-terminus is thought to bind mitochondrial proteins during import. Cytosolic chaperones, in particular, Hsc70 and Hsp90, have been shown to assist with mammalian mitochondrial import, maintaining the newly made protein in a soluble, import-competent state (*23*−*25*). The chaperones that bind the mitochondrial protein dock onto Tom70; the mitochondrial protein is then transferred in an ATP-dependent manner to the core TOM complex for translocation (*24*).

The import of OMM proteins is an active area of investigation, as these proteins appear to use a diverse array of import mechanisms. C-Terminal, tail-anchored OMM proteins, such as Bax and Bcl-xL, which span the OMM once by a transmembrane α-helix, appear to require neither chaperones nor ATP for insertion (*26*). β-Barrel OMM proteins, such as VDAC, require an additional OMM protein complex in addition to the TOM complex, the sorting and assembly machinery (SAM) complex, for correct insertion (*27*−*29*). The proposed mammalian SAM complex proteins include Sam50, the pore-forming protein of the complex, Metaxin 1, which assists with integration of protein into the OMM, and Metaxin 2, a cytosolic protein shown to bind to Metaxin 1 (*30*−*32*). The stoichiometry and stability of the SAM complex have not yet been firmly established. As TSPO appears to span the OMM via five α-helices, it is unknown whether TSPO is inserted directly into the OMM through the TOM complex or requires sorting through the SAM complex.

Previously, the results of Otera et al. (*33*) have shown that TSPO does not use the traditional protein insertion pathway but do not identify the pathway necessary for import. Our results presented herein further these studies by demonstrating that (i) during translocation to the OMM, TSPO interacts with cytosolic chaperones to facilitate an interaction with TOM70, (ii) there are specific amino acids necessary for the targeting of TSPO to the OMM, and (iii) once targeting is complete, insertion of TSPO into the OMM is mediated through Metaxin 1, a member of the SAM complex. Interestingly, the extent of import of TSPO into mitochondria was increased following treatment of hormone-responsive steroidogenic Leydig cells with cAMP, an event that parallels increased levels of cholesterol transport and steroid formation by the cells (*10*). These findings support the existence of a novel three-step integration pathway for OMM proteins and suggest that import of protein into steroid-synthesizing mitochondria might be a cAMP- and thus hormone-regulated process.

MATERIALS AND METHODS

Cell Culture. HeLa cells (Lombardi Comprehensive Cancer Center Cell Culture Facility, Georgetown University), a well-established model used to study import of protein into mitochondria, were maintained in DMEM supplemented with 10% FBS at 37 °C and 6% CO_2. MA-10 mouse tumor Leydig cells, a well-established model for studying transport of cholesterol into mitochondria and steroidogenesis, were a gift from M. Ascoli (University of Iowa, Iowa City, IA) and were maintained in DMEM/Ham's F12 (50:50) supplemented with 5% fetal bovine serum (FBS) and 2.5% horse serum at 37 °C and 3.7% CO_2. In some experiments, confluent MA-10 cells were used to evaluate the effect of cAMP on import into mitochondria. MA-10 cells were treated for 2 h with 1 mM 8-bromo cAMP (Biomol, Farmingdale, NY) prior to mitochondrial isolation.

Plasmid Construction. The mouse TSPO cDNA coding sequence (*5*) was subcloned into pEGFP (CLONTECH Laboratories, Inc., Otsu, Shiga, Japan) at the *Sac*I and *Bam*HI sites (pEGFP-TSPO). For construction of TSPO with a truncated N-terminus, the QuickChange site-directed mutagenesis kit (Stratagene, La Jolla, CA) was used to generate a *Sac*I mutation in the open reading frame of TSPO at the specified region. The vector was then digested with *Sac*I, gel purified, and ligated. TSPO with a C-terminal truncation was generated by creating a sequence-verified stop codon mutation at amino acids 151 and 157. For generating TSPO constructs carrying various deletions, the appropriate regions of TSPO were amplified by polymerase chain reaction (PCR), gel purified, ligated, and reinserted into the pEGFP vector. The fusion sites were verified by sequencing.

Confocal Microscopy. Confocal experiments were performed as stated previously (*34*). Briefly, MA-10 cells were grown on a cover glass bottom dish (Fluorodish, WPI, Sarasota, FL) until 70% confluence. Plasmid constructs were transfected using Lipofectamine 2000 (Invitrogen, Carlsbad, CA). After 24 h, cells were stained with 50 nM Mitotracker CMX (Molecular Probes, Carlsbad, CA) for 30 min and viewed through an Olympus Fluoview FV1000 laser confocal microscope.

Isolation of Mitochondria. Mitochondria were isolated by differential centrifugation as previously described (*35*). Briefly, HeLa cells or confluent MA-10 cells were washed twice with PBS, harvested in buffer A [10 mM Hepes-KOH (pH 7.5), 0.2 M mannitol, 0.07 M sucrose, 1 mM EDTA, and 1× Complete Protease Inhibitor Cocktail Tablets (Roche, Basel, Switzerland)] using a cell lifter, and centrifuged at 500*g* for 10 min. The cell pellet was resuspended in 5 volumes of buffer A, incubated at 4 °C for 10 min, and then centrifuged at 500*g* for 10 min. The cell pellet was resuspended in 5 volumes of buffer B [40 mM Hepes-KOH (pH 7.5), 500 mM sucrose, 160 mM potassium acetate, and 10 mM magnesium acetate, with 1× Complete Protease Inhibitor Cocktail Tablets] and homogenized using an electric potter (glass-Teflon) for 10 passes. Once the process was complete, cells were centrifuged at 500*g* for 10 min. The cell pellet was resuspended in 5 volumes of buffer B with a glass−glass homogenizer (20 passes) and centrifuged at 500*g* for 10 min. The supernatant was pooled and centrifuged at 10000*g* for 10 min at 4 °C to form a mitochondrial pellet. The mitochondrial pellet was resuspended in 1 mL of buffer B and centrifuged at 10000*g* for

10 min to enrich mitochondrial purity. Once the process was complete, the mitochondria were resuspended in mitochondrial import buffer [3% BSA, 250 mM sucrose, 5 mM $MgCl_2$, 80 mM KCl, 10 mM MOPS-KOH (pH 7.2), 5 mM ADP, and 10 mM succinate (Sigma, St. Louis, MO), with 1× Complete Protease Inhibitor Cocktail Tablets] to give a final concentration of 1 mg/mL mitochondria for BN-PAGE import and 5 mg/mL mitochondria for sodium carbonate extraction. Mitochondria were kept on ice until use for no longer than 1 h.

Protein Import. Radiolabeled TSPO was generated using the TNT T7 Quick Coupled Transcription/Translation System (Promega, Madison, WI) in the presence of [^{35}S]methionine (Amersham Biosciences, Piscataway, NJ) as performed previously (*10*) for 1 h at 30 °C. Once complete, the reaction was terminated by the addition of 1 volume of 2×TT buffer [20 mM Hepes-KOH (pH 7.5), 500 mM sucrose, 80 mM KOAc, 5 mM $MgOAc_2$, and 1 mM methionine]. Five microliters of the TNT reaction mixture was added to 50 μg of isolated mitochondria in import buffer for the stated times. Mitochondria were centrifuged at 10000*g* for 10 min, solubilized with 1% digitonin buffer [20 mM Tris-HCl, 0.1 mM EDTA, 50 mM NaCl, 10% (w/v) glycerol, 1% digitonin (Invitrogen), and 1 mM PMSF] for 20 min on ice, and centrifuged at 10000*g* for 10 min. One-half of each sample was digested with 250 μg/mL proteinase K (Qiagen, Dusseldorf, Germany) at 4 °C for 10 min, while the other half of the sample remained untreated.

Blue Native (BN) PAGE. BN-PAGE was performed as described by Simpson (*36*). BN-PAGE loading dye [5% (w/v) Coomassie Brilliant Blue G-250, 500 mM ε-amino-*n*-caproic acid, and 160 mM BisTris (pH 7.0)] was added to the sample supernatants, loaded onto a 4 to 16% native gel (Invitrogen), and run at 34 V overnight. Once the process was complete, the gel was transferred using a semidry transfer apparatus for 1 h at 25 V. The PVDF membrane was then fixed and dried. Then membrane was exposed to a multipurpose phosphor screen for 1−7 days and analyzed by phosphorimaging using the Cyclone Storage Phosphor System (Packard BioScience, Waltham, MA). Once the process was complete, the membrane was then used for immunodetection. Image analysis was performed with Multi Gauge version 3.0 from FujiFilm.

Carbonate Extraction. Mitochondrial protein import was analyzed as described by Fujiki et al. (*37*). After import, mitochondria were incubated at 0.5 mg/mL in 180 μL of 0.1 M Na_2CO_3 (pH 10.5) at 4 °C for 30 min. Forty microliters of sucrose buffer [500 mM sucrose and 0.1 M Na_2CO_3 (pH 10.5)] was added to the top of the sample and centrifuged at 180000*g* for 30 min at 4 °C in a Beckman Coulter TLA-100 rotor. Trichloroacetic acid precipitation was performed on the supernatant, and both pellet and supernatant were analyzed by SDS−PAGE.

Nickel-Sepharose Pull Down Assay. The phosphate carrier (PiC) was also generated from cell free transcription/translation reactions as stated previously (*38*). Radiolabeled TSPO and PiC were diluted 10-fold with reticulocyte lysate and incubated with either geldanamycin or novobiocin. Tom70-H3 was then added to the TNT reaction mixture of either PiC or TSPO (*23*). After 5 min, apyrase was added to terminate the incubation reaction and 50 μL of GTI buffer [100 mM KOAc, 20 mM Hepes-KOH (pH 7.5), 5 mM $MgOAc_2$, 20 mM imidazole, and 0.1% Triton X-100] was added. Nickel-Sepharose slurry was added to the mixture and incubated on an orbital shaker at 4 °C for 30 min. The resulting reaction mixtures contained 5% rectulate lysate of TSPO or PiC containing the nickel-Sepharose slurry. The negative control reaction mixture did not contain Tom70-H3. The positive control did contain geldanamycin (GD), and novobiocin (NB)-treated samples contained 5 μM Tom70-H3 and either 18 μM geldanamycin or 1 mM novobiocin. The beads were then washed twice with GTI buffer and once with GI buffer (lacking Triton X-100). The protein was eluted with 40 μL of LLB with EDTA and separated by SDS−PAGE.

Steroid Biosynthesis. Steroid analysis was preformed as previously described (*34*). Briefly, MA-10 cells were plated in 24-well plates at a density of 50000 cells/well. Cells were transfected after 24 h with various GFP−TSPO constructs. Culture media were collected 24−48 h post-transfection. In certain experiments, cells were washed with serum-free medium and treated with 50 ng/mL hCG for 2 h to determine the hormone responsiveness of the cells. At the end of the incubation, media were collected. To determine maximal steroid production, the hydrosoluble substrate 22(*R*)-hydroxycholesterol (10 μM) was added for 2 h to the cells cultured in serum-free medium. Progesterone production was assessed by RIA in the media. Anti-progesterone antiserum was from MP-Biomedicals (Solon, OH), and [1,2,6,7-^{3}H(N)]progesterone (specific activity of 17.5 Ci/mmol) was from PerkinElmer Life Sciences.

In-Gel Digestion and MS Analysis. Selected protein spots from HeLa extracts separated by BN-PAGE followed by two-dimensional (2D) SDS−PAGE were subjected to an in-gel digestion procedure as described elsewhere (*39*). Resulting in-gel digests were desalted using C18 Zip Tips (Millipore) before analysis by nanoflow reversed-phase liquid chromatography (nanoRPLC) using an Agilent 1100 LC system (Agilent Technologies, Inc., Palo Alto, CA) coupled online to a linear ion trap (LIT) mass spectrometer (LTQ, Thermo Scientific, San Jose, CA). Reversed-phase separations were performed using 75 μm (inside diameter) × 360 μm (outside diameter) × 10 cm (length) capillary columns (Polymicro Technologies Inc., Phoenix, AZ) that were slurry packed in-house with a 5 μm, 300 Å pore size Jupiter C-18 silica-bonded stationary phase (Phenomenex, Torrance, CA). After being injected with 5 μL of sample, the column was washed for 20 min with 98% solvent A [0.1% formic acid in water (v/v)], and peptides were eluted using a linear gradient from 2% solvent B [0.1% formic acid in 100% acetonitrile (v/v)] to 85% solvent B for 110 min at a constant flow rate of 250 nL/min. The LIT-MS instrument was operated in a data-dependent mode in which each full MS scan was followed by seven MS/MS scans where the most abundant peptide molecular ions were dynamically selected for collision-induced dissociation (CID) using a normalized collision energy of 36%. The temperature of the heated capillary and the electrospray voltage (applied on column base) were 180 °C and 1.7 kV, respectively. The CID spectra were searched against a nonredundant human protein database using SEQUEST (Thermo Scientific, San Jose, CA), and results were tabulated for each identified peptide or protein.

Transfection with siRNA. Metaxin 1 siRNAs (5′-GCGCUGUCCUCAGAAUAAACCUGTT-3′, 5′-CGUAAAGAGAAGUAUAAUGCCGACT-3′, and 5′-GGAUAGACGCCAAGAACUAUGUGGA-3′) were purchased from IDT (Coralville, IA) in a TriFecta kit. A hypoxanthine-guanine phosphoribosyltransferase (HPRT)-targeted positive control and a scrambled negative control were obtained from the same provider. MA-10 cells cultured in 100 mm dishes were transfected with 30 μL of Lipofectamine RNAiMAX (Invitrogen) and either the control siRNA duplex or protein-targeted duplexes (20 nM total) for 48 h. At the end of the treatment, the medium was changed, and

Table 1: Primers Used for qPCR Analysis

gene	forward primer	reverse primer	amplicon
Tom40 (NM_001109748)	CGGTGTGGATGGCGAGTACCG	CCTGAACCCACCAAGACATCTG	81
Tom22 (NM_172609)	CGGGCCGAGGAATTACTCCCG	CGTCTTCTTCCAGCTCCTCCTC	64
Tim13 (NM_013898)	CGATAGGCTCCTTGGATAACTCG	AGAGTTGTAGGCGCGGGACAC	98
Tim22 (NM_019818)	GTACCTGGTGGGCGACAAGC	CGAGTCGCTCTTGGCAGGACTCG	85
Sam50 (NM_178614)	GTGCATCCGCTGGTCCTATG	CGGCGTAGTTCAGCTCCAGCCG	77
Metaxin 1 (NM_013604)	CGGTAGAGGAGGAGCCATACCG	TGGATAGAAACGATGCCACTGA	106
Metaxin 2 (NM_016804)	CGTTTGCAGTGGGAAGTGAAACG	CCTGGTCCAGAGTCTTGTTACCC	67
HPRT (NM_013556)	GTACCAGACCTCTCGAAGTGTTGGATAC	TCCAACAACAAACTTGTCTGGAAT	77

3 days later, cells were harvested and mitochondria were isolated for import studies.

Real-Time qPCR. Cells (1×10^5) were harvested from the control and 8-bromo cAMP-treated MA-10 cells and used for RNA isolation to measure mRNA levels. RNA was isolated with an RNeasy Mini Kit (Qiagen) with optional DNase digestion. The cDNA was then generated from the Advantage RT-for-PCR kit (Clontech), using 100 ng of RNA incubated with oligo(dT) primer. Analysis was performed with 7900HT Sequence Detection Agents (Applied Biosystems); the primers are listed in Table 1. TaqMan was from Applied Biosystems (Foster City, CA). All sequences were normalized to HPRT.

Statistics. Statistical analysis was performed using Prism version 4.0 (GraphPad Software, San Diego, CA). Group means were compared using a Student's *t* test or two-way ANOVA test followed by a Bonferroni column test. Data are presented as means ± the standard error of the mean; a p of < 0.05 was considered significant.

Materials. Antibodies specific for TOM22 (Sigma), VDAC, Cox IV, Tom40 (Abcam, Cambridge, MA), Metaxin 1 (BD Bioscience, San Jose, CA), and GapDH (Trevigen, Gaithersburg, MD) were purchased from the various vendors. StAR antibody was a generous gift from D. B. Hales (*40*). A specific rabbit polyclonal antibody was raised against the purified cytosolic fragment of human Tom70 [amino acids 111−608 (J.C.Y., manuscript in preparation)]. The TSPO polyclonal antibody was developed as previously described (*41*).

RESULTS

Import of TSPO. To identify the import pathway of TSPO, we incubated cell-free, radiolabeled, in vitro-translated TSPO with isolated HeLa cell mitochondria and monitored the formation of radiolabeled protein complexes through BN-PAGE by phosphoimaging. We have previously shown that the incubation of TSPO with isolated mitochondria results in import of a fully functional protein, capable of binding and transporting cholesterol in isolated steroidogenic mitochondria from MA-10 cells with consequent generation of steroids (*10*). As the TSPO import reaction with isolated mitochondria proceeded, we observed the presence of a radioactive band migrating at approximately 66 kDa that increased in intensity with incubation time (Figure 1A). Denaturing 2D SDS−PAGE of the BN-PAGE import reactions produced an 18 kDa radioactive band, further confirming import of TSPO into the mitochondria (data not shown). The presence of the TOM complex in the mitochondria was assessed by immunoblot analysis of proteins separated on BN-PAGE gels, electrotransferred on membranes, and blotted using antibodies against Tom22 and Tom40. Both of these antibodies recognized immunoreactive proteins that migrated at 440 kDa, thus indicating the presence of the core TOM complex at the appropriate size, though TSPO was not present in the complex. These data were confirmed in experiments in which the major import receptor Tom20 was knocked down; its absence failed to affect import of TSPO into mitochondria (data not shown). We further probed native membranes with an affinity-purified, anti-TSPO peptide-specific polyclonal antibody. Immunoreactive proteins were shown to migrate at 300 and 800 kDa. It should be noted that HeLa cells are known to have low levels of endogenous TSPO. In parallel studies using the rich-in-TSPO MA-10 cell mitochondria, we identified immunoreactive TSPO at 66, 300, and 800 kDa (data not shown). As mature TSPO is known to form polymers (*42*) and also associate with various other IMM and OMM proteins (*4*, *5*), these large complexes likely contain both homo- and/or heteropolymers of TSPO. The 66 kDa protein complex formed by newly imported TSPO was not detected in HeLa cells by immunoblot analysis as seen for steady-state endogenous TSPO. This may be due to the low levels of TSPO generated by the TNT radiolabeling kit; it must be remembered that TSPO antibodies directed toward the mature peptide are unlikely to recognize protein morphology altered during mitochondrial import.

To confirm import of TSPO into isolated mitochondria, we performed a proteinase K digestion to degrade nonimported proteins. Protein import was performed at 4 and 33 °C, and import reactions were terminated at 0 and 30 min. Samples were then divided into two sets, with and without proteinase K treatment. With the 4 °C import reactions, the amount of 66 kDa complex was greatly reduced relative to that in reactions at 33 °C. Proteinase K digestion of the 4 °C reaction mixtures removed the 66 kDa protein complexes that could be observed in untreated samples (Figure 1B). In contrast, with the permissive 33 °C import reaction, the 66 kDa complex was resistant to proteinase treatment (Figure 1B). These data suggest that the 66 kDa complex, under permissive conditions, is fully incorporated into mitochondrial membranes.

Further confirmation of TSPO membrane integration was obtained by carbonate extraction. Here TSPO was imported under permissive conditions, and mitochondria were purified. These reisolated mitochondria were treated with sodium carbonate to remove proteins that were associated with, but not integrated into, the OMM. Upon carbonate treatment and centrifugation, the majority of TSPO was found in the pellet with the mitochondrial membrane fraction, implying full incorporation of the protein into the OMM (Figure 1C). As a positive control, the carbonate extraction experiment was performed with radiolabeled Tom70, an integral OMM protein, which displayed the same association profile as TSPO (Figure 1C). In contrast, the soluble matrix protein Hsp60 was mostly found in the extracted supernatant fraction. Thus, the HeLa mitochondria have the necessary machinery to drive authentic TSPO import.

TSPO Associates with HSP90 and Tom70. Heat shock proteins (HSPs), including Hsp90, are known to play an important role in delivering proteins to the OMM for import, interacting with Tom70 and assisting translocation in an ATP-dependent manner (*24*). Therefore, to determine if TSPO interacts with Hsp90 for import into the OMM, we incubated the purified C-terminal fragment of Hsp90 (C90) with TSPO. C90 has previously been shown not to interact with mitochondrial proteins before import but does bind stably to Tom70, which outcompetes the Hsp90 interaction and inhibits Tom70-dependent import (*23*). The addition of C90 resulted in a large reduction in the level of TSPO import compared to control (Figure 2A,C), suggesting that import is dependent upon Hsp90 interaction.

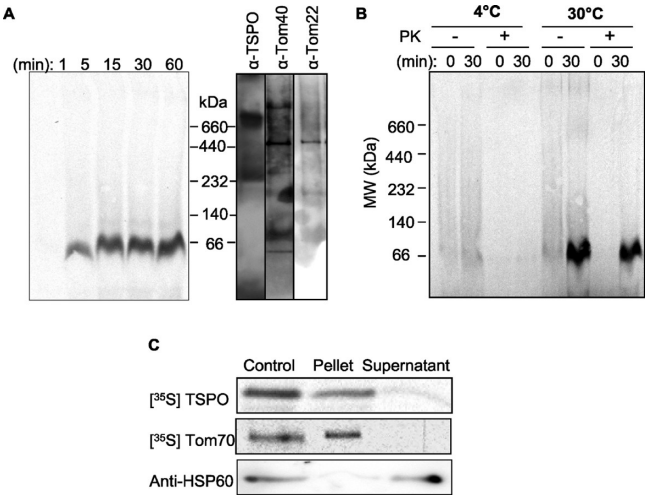

FIGURE 1: Identification of TSPO import complexes in the OMM. (A) Isolated mitochondria from HeLa cells were incubated with in vitro-transcribed/translated [^{35}S]TSPO. The BN-PAGE gel was transferred to PVDF and exposed to a multipurpose phosphor screen (left) or blotted with antisera against TSPO, Tom40, and Tom22 (right). (B) Import of in vitro-transcribed/translated TSPO into mitochondria examined at either 4 or 33 °C; at the stated time points, one-half of the import reaction mixture was treated with proteinase K, and both samples were analyzed by BN-PAGE. (C) In vitro-transcribed/translated [^{35}S]TSPO and [^{35}S]Tom70 were incubated with HeLa cell mitochondria and treated with sodium carbonate for 30 min.

To further test this hypothesis, we performed a series of BN-PAGE experiments. Considering that the chaperone−Tom70 pathway requires ATP for the function of Hsp90 or Hsc70, we depleted ATP from import reaction mixtures using apyrase. BN-PAGE analysis of the samples indicated that the level of the membrane-integrated 66 kDa complex was reduced dramatically in the early stages of import (Figure 2B). As Hsp90 seemed to function in targeting of TSPO to Tom70, we next used the specific Hsp90 inhibitors GD and NB to directly confirm the role of Hsp90 in TSPO import. GD obstructs the N-terminal ATP-binding domain of Hsp90 and inhibits the ATPase activity of the protein, resulting in a stalled complex and a decreased level of translocation across the OMM (*24*, *43*). NB interferes with the targeting of proteins to the mitochondria by binding near the C-terminus of Hsp90, inhibiting substrate binding (*44*). NB also interferes with the docking of Hsp90 to Tom70. As shown in panels B and C of Figure 2, NB and GD significantly reduced the level of import of TSPO compared to control ($p < 0.01$ by ANOVA). NB shows the greatest decrease in the level of import; this is expected as NB would prevent TSPO from binding to Tom70 and associating with the mitochondria. GD is decreased, though not to the same extent as NB, caused by the prevention of cleavage of ATP, thus stalling TSPO on the mitochondrial membrane.

To further confirm that TSPO interacts with Tom70 for import, radiolabeled TSPO was incubated with the His-tagged Tom70 cytosolic fragment and then coprecipitated with nickel-Sepharose, reconstituting the targeting step as previously published. TSPO was recovered from the nickel-Sepharose only when His-tagged Tom70 was present, indicating that TSPO interacts with Tom70 for import (Figure 2D). GD and NB were incubated separately with the His-tagged Tom70 fragment and radiolabeled

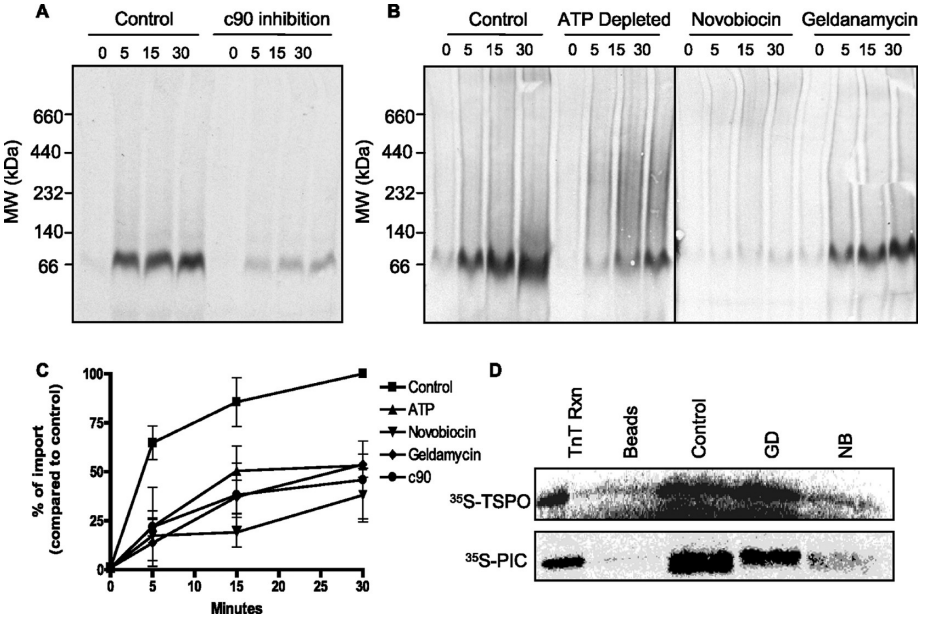

FIGURE 2: TSPO import is dependent upon heat shock proteins and ATP for import. (A) Effects of incubation of C90 with TSPO. TSPO was imported as described above (control). (B) Effect of ATP depletion, 18 μM geldanamycin, and 1 mM novobiocin on TSPO import. (C) Quantification of imported TSPO. Results shown are means ± the standard error of the mean from three independent experiments. (D) Nickel-Sepharose pull-down assay of [^{35}S]TSPO and [^{35}S]PIC. When indicated, geldanamycin or novobiocin was added to the reaction mixture.

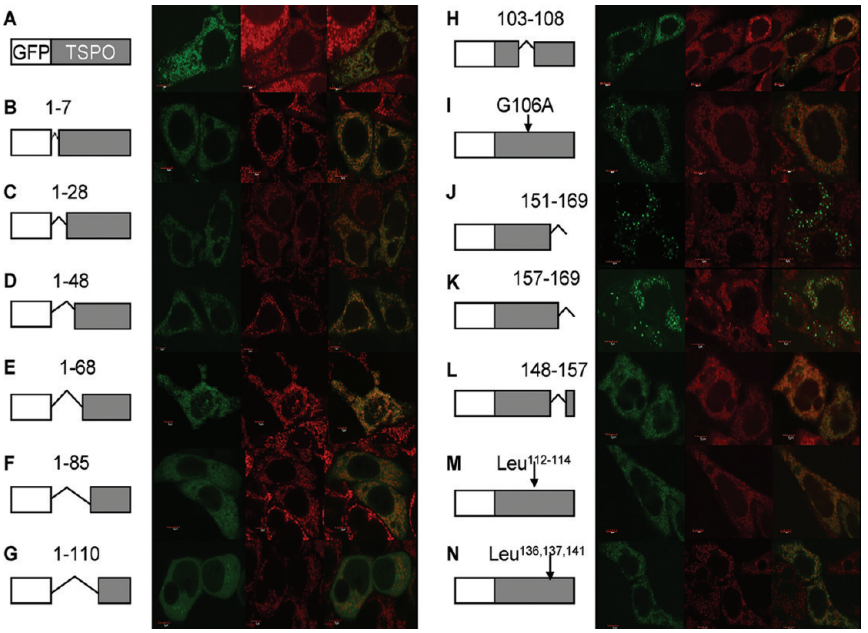

FIGURE 3: Identification of the TSPO amino acid sequence(s) responsible for targeting the protein to the OMM. MA-10 cells were transfected with either wild-type GFP−TSPO fusion protein or various GFP−TSPO constructs, stained with Mitotracker CMX, and visualized by confocal microscopy. Each panel shows the construct used, GFP fluorescence, mitochondrial staining, and the merged image. (A) Wild-type TSPO with GFP linked to the N-terminus. Cells were also transfected with GFP−Δ1−7-TSPO (B), GFP−Δ1−28-TSPO (C), GFP−Δ1−48-TSPO (D), GFP−Δ1−68-TSPO (E), GFP−Δ1−85-TSPO (F), GFP−Δ1−110-TSPO (G), GFP−Δ151−169-TSPO (J), and GFP−Δ157−169-TSPO (K). The cholesterol-binding domain, GFP−Δ148−157-TSPO (L), or the Schellman motif, GFP−Δ103−108-TSPO (H), was removed, and the cells were transfected. Construct GFP−G106A-TSPO (I) with a point mutation altering the Schellman motif and constructs GFP−leucine$^{112-114}$-TSPO (M) and GFP−leucine^{137,138,141}-TSPO (N) were also transfected as described in Materials and Methods.

TSPO, and Tom70-associated material was analyzed. GD did not inhibit the binding of TSPO to Tom70 as the recovery levels were similar to the control (Figure 2D). This finding was similar to that observed with Hsp90-dependent precursor proteins, as GD inhibits only the ATP-dependent release of TSPO from the bound chaperone−Tom70 complex. In contrast, NB did prevent TSPO from associating with Tom70. Again, this finding matched the behavior of Hsp90-dependent precursors. Our results suggest that Hsp90 functions to target TSPO to the Tom70 import receptor by a mechanism typical of the chaperone−Tom70 pathway.

The N-Terminus Is Necessary but Not Sufficient for Targeting TSPO to the Mitochondria. To identify the OMM-targeting sequence(s) of TSPO, we tested the localization of GFP-fused TSPO in MA-10 mouse Leydig cells. TSPO was tagged on either the N- or C-terminus to confirm that the presence of GFP did not interfere with the localization of the protein to mitochondria (data not shown). We then chose a construct in which GFP was linked at the N-terminus of TSPO to ensure that the cholesterol-binding domain on the C-terminus of the protein (*41*, *45*) would not be directly affected by the presence of the GFP moiety. A series of deletion constructs were generated to determine whether the N-terminus is important for mitochondrial targeting (Figure 3). Constructs in which the first 7, 28, 48, 68, and 85 amino acids were removed showed only a slight decrease in the level of TSPO colocalization with the mitochondria, labeled with the Mitotracker CMX dye (Figure 3A−F). Removal of amino acids 1−110 resulted in a loss of colocalization of TSPO with mitochondria and appearance of a diffuse pattern, consistent with an import defect (Figure 3G).

As this region appeared to be necessary for TSPO import, we next examined the importance of amino acids found between residues 88 and 110. A Schellman motif was predicted between amino acids 103 and 108. This motif, often found terminating α-helical secondary structures, is stabilized through hydrophobic interactions between amino acids around a signature glycine residue (*46*). In TSPO, the Schellman motif is predicted to reside in the second intermembrane space loop, bridging the third and fourth predicted transmembrane helices (Figure 4A). Removal of these amino acids (Δ103−108) resulted in focal aggregates of GFP−TSPO in areas adjacent to the mitochondria, as seen through a decrease in the level of colocalization with Mitotracker (Figure 3H). The point mutation of glycine 106 to alanine (G106A), which disrupts the Schellman motif by reducing flexibility, resulted in a similar profile as seen with Δ103−108-TSPO (Figure 3I). The Schellman motif between amino acids 103 and 108 of TSPO thus appears to be critical for proper folding and/or membrane insertion. Though its role in localization and import remains open to investigation, the juxtamitochonrial location of aggregates suggests that the proteins are targeted, but not capable of import.

The C-Terminus Is Necessary for Targeting to the OMM. As roughly two-thirds of the TSPO protein from the N-terminus can be removed without an effect the localization of the remaining protein to mitochondria, we then questioned whether the removal of the C-terminus affects TSPO localization. Generation of Δ151−169 and Δ157−169 amino acid deletion constructs caused a decrease in the degree of localization of the protein to mitochondria with an increase in the level of aggregation of GFP−TSPO (Figure 3J,K). Considering that the cholesterol-binding domain of TSPO is present within the deleted region in Δ151−169-TSPO, it was possible that this domain could play a role in the targeting of TSPO to the OMM. However, removal of the region of residues 148−157, which contains the cholesterol-binding domain, did not alter the TSPO/mitochondria colocalization pattern (Figure 3L), suggesting that

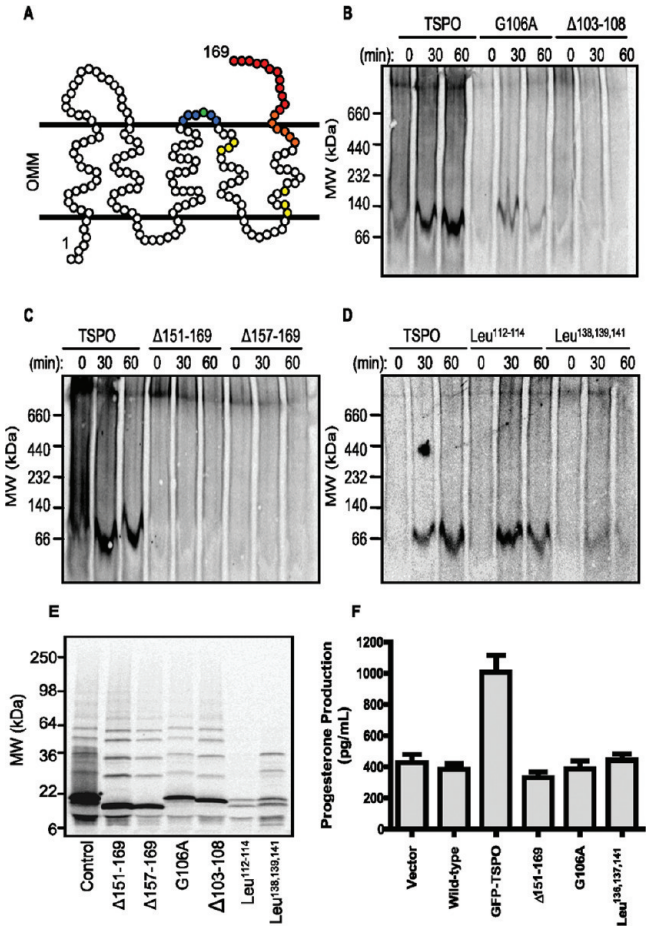

FIGURE 4: TSPO protein regions and amino acids required for insertion into the OMM. (A) Model of the 18 kDa TSPO protein present in the OMM. Blue amino acids represent the C-terminus; red amino acids represent the mutated leucine residues, and green amino acids show the Schellman motif with the yellow amino acid in the middle representing the mutated glycine. (B) Schellman motif mutants of the TSPO protein were compared with wild-type TSPO for import into HeLa cell mitochondria, followed by analysis by BN-PAGE. (C) Effect of removal of the C-terminus with constructs Δ157−169 and Δ151−169 on inhibition of import of TSPO into isolated mitochondria. (D) Effect of leucine mutations on import of in vitro-transcribed/translated radiolabeled TSPO into HeLa cell mitochondria. (E) SDS−PAGE of radiolabeled constructs from import studies for confirmation of size due to mutations. (F) Measurement of progesterone production produced by MA-10 was performed as stated in Materials and Methods. Results shown are means ± the standard error of the mean from three independent experiments ($n = 9$).

the domain does not play a role in TSPO import. Because the degree of TSPO/mitochondria colocalization decreases with the removal of the C-terminus and although the cholesterol-binding domain plays no role, it could be that some other feature of the C-terminus, such as the overall secondary structure, could play a role in TSPO localization with the OMM. A comparison of the Schellman motif and C-terminal sequences was made, revealing two conserved areas of high leucine content, amino acids 112−114 and 136, 137, and 141 (Figure 4A). Point mutations of both sets of leucines (leucine$^{112-114}$ and leucine^{136,137,141}) into alanines did not alter TSPO colocalization with mitochondria (Figure 3M,N).

Inhibition of Import of TSPO Mutants. In the GFP−TSPO/mitochondria colocalization experiments described above, several constructs exhibited reduced degrees of colocalization. To confirm that a reduced level of colocalization reflects a reduced level of import of TSPO into mitochondria, BN-PAGE of in vitro import reactions was performed using [^{35}S]TSPO mutant constructs. Notably, the Schellman motif mutant Δ103−108 could not be imported into the 66 kDa complex (Figure 4B). The import of TSPO carrying the G106A point mutation also resulted in the greatly decreased level of import of the 66 kDa protein complex, although not to the extent seen with the Δ103−108-TSPO construct (Figure 4B). The ability to import was then tested for the TSPO constructs in which the C-terminal domains, residues 151−169 and 157−169, were removed. Both deletions clearly abolished the import of the 66 kDa complex in isolated mitochondrial (Figure 4C). To determine whether the alteration of the structure of the C-terminus results in the inhibition of TSPO import, the leucine$^{112-114}$ and leucine^{136,137,141} TSPO point mutants were analyzed by BN-PAGE. Leucine$^{112-114}$ did not show an effect on TSPO import (Figure 4D). However, the leucine^{136,137,141} TSPO mutant showed a significant decrease in the level of import of the 66 kDa complex (Figure 4D), although its level of synthesis in vitro was similar to that of the leucine$^{112-114}$ mutant (Figure 4E). This result differs from the results of confocal microscopy in which the leucine$^{112-114}$ TSPO mutant was found to colocalize with mitochondria. This apparent discrepancy could be due to differences between the in situ and in vitro situations, including the highly concentrated intracellular environment, which favor TSPO import and alleviate partial import defects. Overall, the in vitro and live cell results support an important role of the Schellman motif and sequences within the C-terminus of TSPO for import.

Functional Evaluation of TSPO Import in Steroid Biosynthesis. As TSPO controls the rate-limiting step in the production of steroids, tranport of cholesterol into mitochondria, increasing the TSPO protein concentration in the OMM by transient transfection with a TSPO construct was shown to increase the level of progesterone production by MA-10 mouse Leydig cells in culture (*34*). To investigate the functional role of altered import of TSPO mutants previously evaluated by confocal microscopy and BN-PAGE analyses, we measured the level of progesterone production in MA-10 cells transfected with wild-type and mutated TSPO constructs (Figure 4). As the constitutive expression of TSPO in MA-10 cells was not silenced, a basal level of progesterone production was observed. However, transfection of MA-10 cells with GFP−TSPO resulted in a marked 2.5-fold increase in the level of progesterone production (Figure 4F; $p < 0.01$ by a Student's t test), consistent with previous findings (*34*). Transfection with TSPO in which the Schellman motif was mutated (G106A) did not affect basal progesterone formation but did not cause a similar increase seen by transfection with wild-type GFP−TSPO. The results obtained with the G106A-TSPO mutant support the data obtained in situ by confocal microscopy and in vitro using BN-PAGE, indicating that such mutants are not imported and therefore not functional in cholesterol transport. The leucine^{136,137,141} mutant showed progesterone levels near basal levels, suggesting that while this mutant may be imported into the OMM, it was not functional in the transport of cholesterol into the mitochondrial matrix. C-Terminal mutants also failed to increase the level of progesterone production, consistent with an import defect. The finding that removal of the cholesterol-binding domain in the Δ151−169-TSPO construct resulted in a reduction in the basal level of progesterone production is in agreement with previous findings (*10*, *45*).

Metaxin 1 Is Necessary for TSPO Import. Considering the data presented above which show that TSPO does not stably

Table 2: Identification of Proteins Present in the 66 and 800 kDa HeLa Protein Complexes by Mass Spectrometry[a]

protein	sequences identified
66 kDa	
Metaxin 1	RSLASPGISPGPLTATIG-GAVAGGGPR
nonspecific lipid-transfer protein	K.LQNLQLQPGNAKL
	K.IGGIFAFK.V
	K.ANLVFKEIEK.K
voltage-dependent anion channel (VDAC 1)	TDEFQLHTNVNDGTEFG-GSIYQK
	R.WTEYGLTFTEK.W
	K.LTFDSSFSPNTGK.K
800 kDa	
adenine nucleotide translocator (ANT 1,2,3)	K.LLLQVQHASK.Q
	R.YFPTQALNFAFK.D
	R.AAYFGIYDTAK.G
	K.DFLAGGIAAAISK.T
apolipoprotein A-I	K.VSFLSALEEYTK.K
apolipoprotein A-II	K.SPELQAEAK.S
fatty acid synthase	K.VVVQVLAEEPEAVLK.G
	R.LQVVDQPLPVR.G
	K.VGDPQELNGITR.A
mitofilin	R.ELDSITPEVLPGWK.G
voltage-dependent anion channel (VDAC 1,3)	R.VTQSNFAVGYK.T
	K.LSQNNFALGYK.A
annexin A2	K.SALSGHLETVILGLLK.T
	R.QDIAFAYQR.R
	K.TPAQYDASELK.A
	K.GVDEVTIVNILTNR.S

[a] The imported 66 kDa TSPO complex and the endogenous 800 kDa mitochondrial protein complex separated by BN-PAGE and 2D SDS−PAGE were analyzed by mass spectrometry; some of the major identified proteins are listed.

associate with the core TOM complex during import, we undertook a detailed analysis of the identification of proteins involved. Using a combination of BN-PAGE and 2D SDS−PAGE followed by mass spectrometric analysis of proteins present in all spots separated from the 66 kDa complex, as well as the stable 800 kDa complex, we identified a number of proteins of interest (Table 2). Among the identified proteins present in the 66 kDa protein complex was Metaxin 1. Metaxin 1 was shown previously to be present in MA-10 cells and induced by hormone treatment in a manner parallel to steroid synthesis (*47*). Probing BN-PAGE immunoblots with an anti-Metaxin 1 antibody showed that the protein identified migrated at a molecular size similar to that of [^{35}S]TSPO (Figure 5A).

Metaxin 1 is the mammalian homologue of yeast Sam37 (also called Mas37/Tom37), a component of the SAM complex known to function in the stable integration of OMM β-barrel proteins (*29*, *32*). Metaxin 1's primary role in the OMM is to function as a receptor in the SAM complex (*48*) It was possible that Metaxin 1 could play a role in TSPO import, and to address this, an siRNA duplex that targets Metaxin 1 was used to knock down its level of expression. Mitochondria were isolated from MA-10 cells that had been treated for 5 days with either a siRNA complex toward Metaxin 1 or a scrambled negative control (each at 20 nM). Figure 5C shows that the siRNA successfully reduced Metaxin 1 protein levels compared to the scrambled siRNA control. Moreover, the basal levels of the inner mitochondrial membrane protein COXIV were unaffected by Metaxin 1 silencing, though endogenous TSPO levels were slightly decreased. BN-PAGE of import into the mitochondria from Metaxin 1 knock down cells showed that the rate of TSPO import at the 66 kDa complex was diminished, compared to that in mitochondria from scrambled siRNA and untreated cells (Figure 5B). These data, quantified in Figure 5D ($p < 0.05$ by ANOVA), suggest that Metaxin 1 is involved in import of TSPO into the OMM.

Cyclic AMP-Stimulated Mitochondria Increase the Level of TSPO Import. Steroidogenesis is initiated upon the transfer of cholesterol from the OMM to the IMM where it interacts with CYP11A1 to be converted into pregnenolone. This transfer of cholesterol is activated via a cAMP-dependent pathway, resulting in an increase in the level of protein synthesis, protein phosphorylation, and lipid synthesis (*49*). To determine if activation of steroidogenesis would alter mitochondrial protein import, MA-10 cells were incubated with 1 mM cAMP for 2 h, the point at which maximal rates of steroid production are seen in vitro, and the mitochondria were isolated (*34*). Upon initiation of TSPO mitochondrial import, a 1.7-fold increase in the level of 66 kDa TSPO was observed in mitochondria isolated from cAMP-treated cells within the first 5 min followed by 2.2- and 1.8-fold increases in the level of induction over basal at 15 and 30 min, respectively (Figure 6A,B). The effect of cAMP was statistically significant ($p < 0.05$ by a Student's t test). To determine if gene and protein expression levels were altered, both qPCR and Western blot analysis were performed. qPCR results showed no increase upon cAMP treatment of the Tom40 pore for OMM protein import and Tim22 for IMM protein import. Metaxin 1 showed a slight but not significant increase upon cAMP stimulation (Figure 6C). While the 2 h cAMP treatment is too short for most transcriptionally based changes in protein expression, translation- or degradation-based regulation can cause faster effects. However, upon immunoblot analysis, there were no significant increases seen in any mitochondrial protein, including Metaxin 1 (Figure 6D). The level of expression of StAR protein, which is a cAMP-induced protein, was also measured to confirm the 8-bromo cAMP activity. StAR mRNA levels were increased by 10-fold (data not shown), and there was also a pronounced induction of StAR protein levels (Figure 6D). This suggests that while the mechanisms necessary for mitochondrial import are being upregulated, the increase in the level of TSPO import is not due to an increase in the level of mitochondrial import proteins. It is possible, however, that changes in the composition of protein complexes and protein−protein interactions needed for import could occur.

DISCUSSION

In the experiments described above, we determined the pathway for the targeting and insertion of the multimembrane spanning protein, TSPO, into the OMM. A schematic representation of the steps of the process is shown in Figure 7. The initial targeting of TSPO to mitochondria has been shown to be dependent on the presence of the cytosolic chaperones Hsp90 and most likely Hsc70 as well as their interactions with Tom70 upon arrival at the OMM. As this first step shows, these early interactions of the cytosolic chaperones and Tom70 depend on the proper binding of TSPO to the chaperones. Targeting of chaperone−TSPO complexes to Tom70 is the second step. The Tom70 complex formed at this stage may be relatively unstable, and although not detected via BN-PAGE, it can be reconstituted

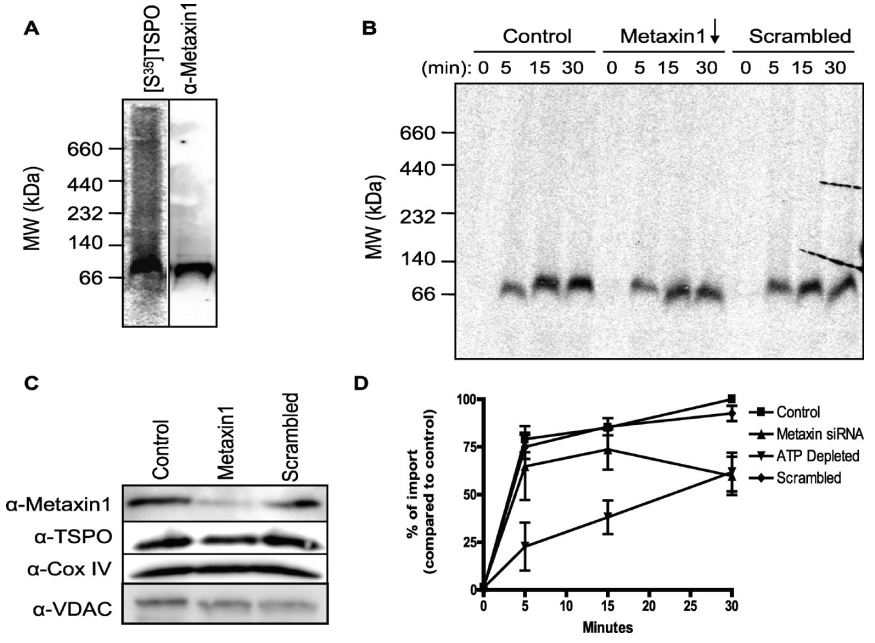

FIGURE 5: TSPO import is dependent on Metaxin 1. (A) MA-10 mitochondria incubated with in vitro-transcribed/translated TSPO analyzed by BN-PAGE, and blotted with anti-Metaxin 1 antibody. (B) In vitro-transcribed/translated TSPO incubated with mitochondria isolated from MA-10 control cells, Metaxin 1-depleted cells, and MA-10 cells treated with scrambled siRNAs. (C) Immunoblot analysis for Metaxin 1, COX IV, TSPO, and VDAC in mitochondria isolated form MA-10 cells treated with the various siRNAs. (D) Quantification of imported TSPO. Results shown are means ± the standard error of the mean from three independent experiments.

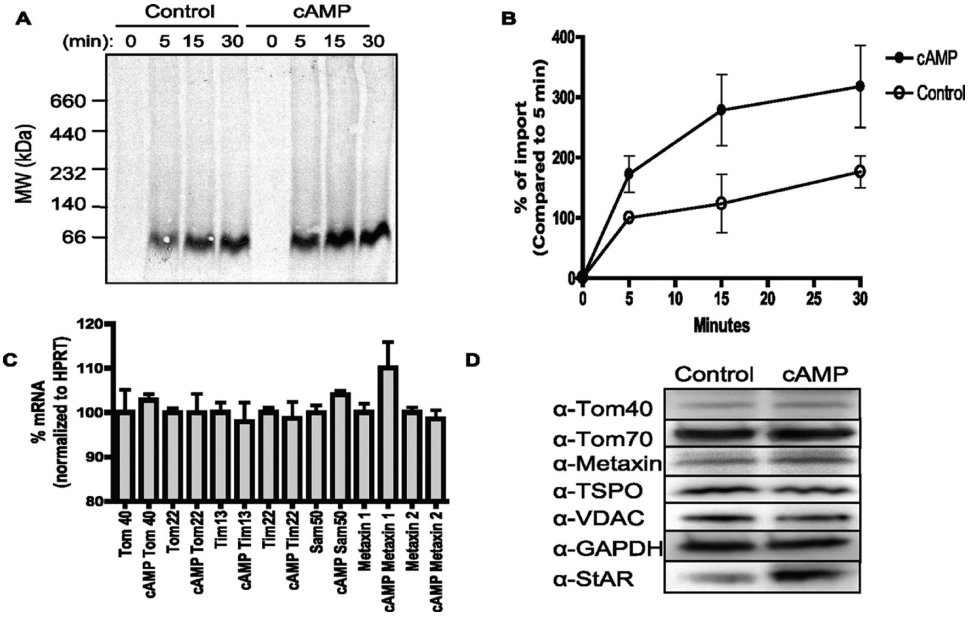

FIGURE 6: TSPO import enhanced with cAMP-stimulated mitochondria. (A) Mitochondria isolated from MA-10 cells incubated with or without 1 mM cAMP were incubated with radiolabeled TSPO and analyzed via BN-PAGE. (B) Quantification of imported TSPO. Results shown are means ± the standard error of the mean from three independent experiments. (C) RT-qPCR analysis of MA-10 RNA with or without 1 mM cAMP. (D) Immunoblot analysis of MA-10 cells incubated with and without 1 mM 8-bromo-AMP.

with purified Tom70. The third step of import of TSPO into the OMM is insertion into the membrane. This is a temperature- and ATP-dependent process involving the release of TSPO from the chaperones and Tom70. Metaxin 1 functions at this step to boost the kinetics of insertion. After insertion, TSPO becomes resistant to proteinase K. The third step requires formation of specific secondary structures, including the Schellman motif, which probably aids integration of the third and fourth transmembrane domains of TSPO into the OMM. In steroidogenic and hormone-responsive MA-10 Leydig cells, the rate of import into the isolated mitochondria can be accelerated following treatment with cAMP (Figure 7, yellow arrow). These conformational requirements suggest that the 66 kDa complex contains TSPO in a native folded state. The native complex is most likely a homo-oligomer of TSPO as has previously been observed. The 66 kDa complex then matures into the final complexes of up to 800 kDa which are observed in steady-state mitochondria of endogenous TSPO. These complexes may include the known TSPO interacting proteins VDAC and ANT, further identified by mass spectrometry to be present in this complex, as well as other

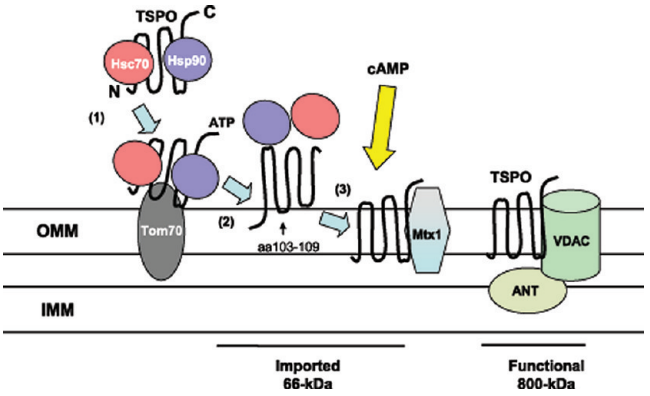

FIGURE 7: Import of TSPO into the OMM. We have outlined the steps necessary for TSPO targeting and insertion into the OMM. (1) TSPO is targeted to the OMM through its interactions with cytosolic chaperones, Hsc70 and Hsp90. (2) At the OMM, TSPO interacts with Tom70 and is released from the chaperones in an ATP-dependent manner. (3) Insertion of TSPO into the OMM is dependent upon Metaxin 1 (Mtx1) and TSPO structure, where both the C-terminus and the Schellman motif (amino acids 103−108) are necessary to form a 66 kDa complex. Once import is complete, TSPO associates with other protein complexes found in the OMM identified previously as VDAC and ANT. The yellow arrow indicates the possible step accelerated by cAMP treatment.

proteins. This process of TSPO import constitutes a novel pathway for import of protein into the OMM.

As mentioned earlier, our results broadly support the conclusion of Otera et al. (*33*) that TSPO is inserted into mitochondria via a novel pathway. The authors identified a 66 kDa TSPO complex by BN-PAGE upon import into HeLa mitochondria. They also demonstrated that Tom22, Tom20, Tom40, and Sam50 were not involved in TSPO import whereas Tom70 played a role in targeting of TSPO to mitochondria, in agreement with our findings. They hypothesized the importance of other unidentified mitochondrial proteins for TSPO and other protein import. We now confirm these findings and extend them by providing evidence that Hsp90 and Metaxin 1 also function in the targeting and insertion of TSPO into the OMM. Although the role of heat shock proteins in TSPO mitochondrial import was previously discussed, the interaction was described as ATP-independent, a conclusion that is not supported by our data. Our demonstration of ATP-dependent import is in fact consistent with established work on the Tom70 pathway and with current models of Hsp90 and Hsc70 activity.

We furthermore report that Metaxin 1 and the C-terminus of TSPO are critical for insertion of TSPO into the OMM. These findings might explain the mechanism of import of a number of proteins into the OMM. Sam37 has been shown to play a role in the import of α-helical, C-terminally targeted TOM proteins, such as Tom22 and small Tom proteins. This finding suggests that the interaction of TSPO via its C-terminus with Metaxin 1 is necessary for its complete import into the OMM. Slight alteration of the α-helix of the C-terminus could interfere with this import, as seen with the inhibition of leucine[136,137,141] mutant import by BN-PAGE. Metaxin 2, a cytosolic protein shown to interact with Metaxin 1 at the OMM, could also play a role in import. Moreover, we identified the amino acids critical for insertion of the protein into the OMM and demonstrated the functional significance of insertion and import of TSPO into mitochondria of steroidogenic cells in which TSPO, a cholesterol-binding protein, functions in cholesterol import, the rate-determining step in steroid biosynthesis.

The final step of TSPO import is the functional integration into the OMM. Antibody detection of TSPO on the BN gel membrane identified a major 800 kDa complex while not recognizing the protein migrating at 66 kDa in HeLa cells either due to limited amounts of the protein or due to the accessibility of the antibody to the antigen. We propose that the 800 kDa complex represents the biologically functional population of TSPO in the OMM. Mass spectrometric analysis of these complexes revealed that at the 66 kDa complex in HeLa cells, in addition to Metaxin 1, VDAC1 was identified. As Metaxin 1 assists with insertion of the β-barrel protein into the OMM, it is possible the close association of TSPO with VDAC could form here, allowing a foundation for a larger protein complex to form. Mass spectrometric analysis of the 800 kDa complex identified the isoforms of VDAC and ANT. As it is known that TSPO physically and functionally interacts with VDAC (*4*, *5*, *34*) and ANT (*5*) and that they are part of MPTP (*15*), we propose that these complexes represent the contact sites between the OMM and the IMM, a place where TSPO is concentrated (*7*). As contact sites have been suggested to play a role in cholesterol transport, apoptosis, energy metabolism, and protein transport, improving our understanding of the proteins involved in this area could lead to a deeper understanding of the function of contact sites (*50*−*52*). Interestingly, at the 800 kDa protein complex, mass spectrometry identified other known mitochondrial proteins, that is, fatty synthase and apolipoprotein A-I and A-II, likely participating in the transport of cholesterol into mitochondria, needed for steroid formation in steroidogenic cells and membrane biogenesis in proliferating cells.

In conclusion, the findings reported here using as a model TSPO support the existence of a novel three-step integration pathway for OMM proteins and suggest that such protein import might be a cAMP-regulated process.

ACKNOWLEDGMENT

We thank Dr. M. Ascoli (University of Iowa) for the MA-10 Leydig cell line, Dr. D. B. Hales (University of Chicago) for the anti-StAR antiserum, and the National Hormone and Pituitary Program (National Institute of Diabetes and Digestive and Kidney Diseases, National Institutes of Health, Bethesda, MD) for the hCG.

REFERENCES

1. Papadopoulos, V., Baraldi, M., Guilarte, T. R., Knudsen, T. B., Lacapere, J. J., Lindemann, P., Norenberg, M. D., Nutt, D., Weizman, A., Zhang, M. R., and Gavish, M. (2006) Translocator protein (18 kDa): New nomenclature for the peripheral-type benzodiazepine receptor based on its structure and molecular function. *Trends Pharmacol. Sci. 27*, 402–409.
2. Lacapere, J. J., and Papadopoulos, V. (2003) Peripheral-type benzodiazepine receptor: Structure and function of a cholesterol-binding protein in steroid and bile acid biosynthesis. *Steroids 68*, 569–585.
3. Murail, S., Robert, J. C., Coic, Y. M., Neumann, J. M., Ostuni, M. A., Yao, Z. X., Papadopoulos, V., Jamin, N., and Lacapere, J. J. (2008) Secondary and tertiary structures of the transmembrane domains of the translocator protein TSPO determined by NMR. Stabilization of the TSPO tertiary fold upon ligand binding. *Biochim. Biophys. Acta 1778*, 1375–1381.
4. McEnery, M. W., Snowman, A. M., Trifiletti, R. R., and Snyder, S. H. (1992) Isolation of the mitochondrial benzodiazepine receptor: Association with the voltage-dependent anion channel and the adenine nucleotide carrier. *Proc. Natl. Acad. Sci. U.S.A. 89*, 3170–3174.
5. Garnier, M., Dimchev, A. B., Boujrad, N., Price, J. M., Musto, N. A., and Papadopoulos, V. (1994) In vitro reconstitution of a functional peripheral-type benzodiazepine receptor from mouse Leydig tumor cells. *Mol. Pharmacol. 45*, 201–211.

6. Veenman, L., Shandalov, Y., and Gavish, M. (2008) VDAC activation by the 18 kDa translocator protein (TSPO), implications for apoptosis. *J. Bioenerg. Biomembr. 40*, 199–205.
7. Culty, M., Li, H., Boujrad, N., Amri, H., Vidic, B., Bernassau, J. M., Reversat, J. L., and Papadopoulos, V. (1999) In vitro studies on the role of the peripheral-type benzodiazepine receptor in steroidogenesis. *J. Steroid Biochem. Mol. Biol. 69*, 123–130.
8. Galiegue, S., Tinel, N., and Casellas, P. (2003) The peripheral benzodiazepine receptor: A promising therapeutic drug target. *Curr. Med. Chem. 10*, 1563–1572.
9. Galiegue, S., Casellas, P., Kramar, A., Tinel, N., and Simony-Lafontaine, J. (2004) Immunohistochemical assessment of the peripheral benzodiazepine receptor in breast cancer and its relationship with survival. *Clin. Cancer Res. 10*, 2058–2064.
10. Hauet, T., Yao, Z. X., Bose, H. S., Wall, C. T., Han, Z., Li, W., Hales, D. B., Miller, W. L., Culty, M., and Papadopoulos, V. (2005) Peripheral-type benzodiazepine receptor-mediated action of steroidogenic acute regulatory protein on cholesterol entry into Leydig cell mitochondria. *Mol. Endocrinol. 19*, 540–554.
11. Wright, G., and Reichenbecher, V. (1999) The effects of superoxide and the peripheral benzodiazepine receptor ligands on the mitochondrial processing of manganese-dependent superoxide dismutase. *Exp. Cell Res. 246*, 443–450.
12. Falchi, A. M., Battetta, B., Sanna, F., Piludu, M., Sogos, V., Serra, M., Melis, M., Putzolu, M., and Diaz, G. (2007) Intracellular cholesterol changes induced by translocator protein (18 kDa) TSPO/PBR ligands. *Neuropharmacology 53*, 318–329.
13. Levin, E., Premkumar, A., Veenman, L., Kugler, W., Leschiner, S., Spanier, I., Weisinger, G., Lakomek, M., Weizman, A., Snyder, S. H., Pasternak, G. W., and Gavish, M. (2005) The peripheral-type benzodiazepine receptor and tumorigenicity: Isoquinoline binding protein (IBP) antisense knockdown in the C6 glioma cell line. *Biochemistry 44*, 9924–9935.
14. Shoukrun, R., Veenman, L., Shandalov, Y., Leschiner, S., Spanier, I., Karry, R., Katz, Y., Weisinger, G., Weizman, A., and Gavish, M. (2008) The 18-kDa translocator protein, formerly known as the peripheral-type benzodiazepine receptor, confers proapoptotic and antineoplastic effects in a human colorectal cancer cell line. *Pharmacogenet. Genomics 18*, 977–988.
15. Veenman, L., Papadopoulos, V., and Gavish, M. (2007) Channel-like functions of the 18-kDa translocator protein (TSPO): Regulation of apoptosis and steroidogenesis as part of the host-defense response. *Curr. Pharm. Des. 13*, 2385–2405.
16. Stojanovski, D., Johnston, A. J., Streimann, I., Hoogenraad, N. J., and Ryan, M. T. (2003) Import of nuclear-encoded proteins into mitochondria. *Exp. Physiol. 88*, 57–64.
17. Rehling, P., Brandner, K., and Pfanner, N. (2004) Mitochondrial import and the twin-pore translocase. *Nat. Rev. Mol. Cell Biol. 5*, 519–530.
18. Neupert, W., and Herrmann, J. M. (2007) Translocation of proteins into mitochondria. *Annu. Rev. Biochem. 76*, 723–749.
19. Rapaport, D. (2003) Finding the right organelle. Targeting signals in mitochondrial outer-membrane proteins. *EMBO Rep. 4*, 948–952.
20. Rapaport, D. (2005) How does the TOM complex mediate insertion of precursor proteins into the mitochondrial outer membrane?. *J. Cell Biol. 171*, 419–423.
21. Kunkele, K. P., Heins, S., Dembowski, M., Nargang, F. E., Benz, R., Thieffry, M., Walz, J., Lill, R., Nussberger, S., and Neupert, W. (1998) The preprotein translocation channel of the outer membrane of mitochondria. *Cell 93*, 1009–1019.
22. Chan, N. C., Likic, V. A., Waller, R. F., Mulhern, T. D., and Lithgow, T. (2006) The C-terminal TPR domain of Tom70 defines a family of mitochondrial protein import receptors found only in animals and fungi. *J. Mol. Biol. 358*, 1010–1022.
23. Young, J. C., Hoogenraad, N. J., and Hartl, F. U. (2003) Molecular chaperones Hsp90 and Hsp70 deliver preproteins to the mitochondrial import receptor Tom70. *Cell 112*, 41–50.
24. Fan, A. C., Bhangoo, M. K., and Young, J. C. (2006) Hsp90 functions in the targeting and outer membrane translocation steps of Tom70-mediated mitochondrial import. *J. Biol. Chem. 281*, 33313–33324.
25. Bhangoo, M. K., Tzankov, S., Fan, A. C., Dejgaard, K., Thomas, D. Y., and Young, J. C. (2007) Multiple 40-kDa heat-shock protein chaperones function in Tom70-dependent mitochondrial import. *Mol. Biol. Cell 18*, 3414–3428.
26. Lan, L., Isenmann, S., and Wattenberg, B. W. (2000) Targeting and insertion of C-terminally anchored proteins to the mitochondrial outer membrane is specific and saturable but does not strictly require ATP or molecular chaperones. *Biochem. J. 349*, 611–621.
27. Paschen, S. A., Neupert, W., and Rapaport, D. (2005) Biogenesis of β-barrel membrane proteins of mitochondria. *Trends Biochem. Sci. 30*, 575–582.
28. Pfanner, N., Wiedemann, N., Meisinger, C., and Lithgow, T. (2004) Assembling the mitochondrial outer membrane. *Nat. Struct. Mol. Biol. 11*, 1044–1048.
29. Kozjak-Pavlovic, V., Ross, K., Benlasfer, N., Kimmig, S., Karlas, A., and Rudel, T. (2007) Conserved roles of Sam50 and metaxins in VDAC biogenesis. *EMBO Rep. 8*, 576–582.
30. Kozjak, V., Wiedemann, N., Milenkovic, D., Lohaus, C., Meyer, H. E., Guiard, B., Meisinger, C., and Pfanner, N. (2003) An essential role of Sam50 in the protein sorting and assembly machinery of the mitochondrial outer membrane. *J. Biol. Chem. 278*, 48520–48523.
31. Armstrong, L. C., Saenz, A. J., and Bornstein, P. (1999) Metaxin 1 interacts with metaxin 2, a novel related protein associated with the mammalian mitochondrial outer membrane. *J. Cell. Biochem. 74*, 11–22.
32. Armstrong, L. C., Komiya, T., Bergman, B. E., Mihara, K., and Bornstein, P. (1997) Metaxin is a component of a preprotein import complex in the outer membrane of the mammalian mitochondrion. *J. Biol. Chem. 272*, 6510–6518.
33. Otera, H., Taira, Y., Horie, C., Suzuki, Y., Suzuki, H., Setoguchi, K., Kato, H., Oka, T., and Mihara, K. (2007) A novel insertion pathway of mitochondrial outer membrane proteins with multiple transmembrane segments. *J. Cell Biol. 179*, 1355–1363.
34. Liu, J., Rone, M. B., and Papadopoulos, V. (2006) Protein-protein interactions mediate mitochondrial cholesterol transport and steroid biosynthesis. *J. Biol. Chem. 281*, 38879–38893.
35. Krueger, K. E., and Papadopoulos, V. (1990) Peripheral-type benzodiazepine receptors mediate translocation of cholesterol from outer to inner mitochondrial membranes in adrenocortical cells. *J. Biol. Chem. 265*, 15015–15022.
36. Simpson, R. J. (2003) Proteins and proteomics: A laboratory manual , Cold Spring Harbor Laboratory Press, Plainview, NY.
37. Fujiki, Y., Hubbard, A. L., Fowler, S., and Lazarow, P. B. (1982) Isolation of intracellular membranes by means of sodium carbonate treatment: Application to endoplasmic reticulum. *J. Cell Biol. 93*, 97–102.
38. Zara, V., Palmieri, F., Mahlke, K., and Pfanner, N. (1992) The cleavable presequence is not essential for import and assembly of the phosphate carrier of mammalian mitochondria but enhances the specificity and efficiency of import. *J. Biol. Chem. 267*, 12077–12081.
39. Wilm, M., Shevchenko, A., Houthaeve, T., Breit, S., Schweigerer, L., Fotsis, T., and Mann, M. (1996) Femtomole sequencing of proteins from polyacrylamide gels by nano-electrospray mass spectrometry. *Nature 379*, 466–469.
40. Hales, K. H., Diemer, T., Ginde, S., Shankar, B. K., Roberts, M., Bosmann, H. B., and Hales, D. B. (2000) Diametric effects of bacterial endotoxin lipopolysaccharide on adrenal and Leydig cell steroidogenic acute regulatory protein. *Endocrinology 141*, 4000–4012.
41. Li, H., Yao, Z., Degenhardt, B., Teper, G., and Papadopoulos, V. (2001) Cholesterol binding at the cholesterol recognition/interaction amino acid consensus (CRAC) of the peripheral-type benzodiazepine receptor and inhibition of steroidogenesis by an HIV TAT-CRAC peptide. *Proc. Natl. Acad. Sci. U.S.A. 98*, 1267–1272.
42. Delavoie, F., Li, H., Hardwick, M., Robert, J. C., Giatzakis, C., Peranzi, G., Yao, Z. X., Maccario, J., Lacapere, J. J., and Papadopoulos, V. (2003) In vivo and in vitro peripheral-type benzodiazepine receptor polymerization: Functional significance in drug ligand and cholesterol binding. *Biochemistry 42*, 4506–4519.
43. Young, J. C., and Hartl, F. U. (2000) Polypeptide release by Hsp90 involves ATP hydrolysis and is enhanced by the co-chaperone p23. *EMBO J. 19*, 5930–5940.
44. Marcu, M. G., Chadli, A., Bouhouche, I., Catelli, M., and Neckers, L. M. (2000) The heat shock protein 90 antagonist novobiocin interacts with a previously unrecognized ATP-binding domain in the carboxyl terminus of the chaperone. *J. Biol. Chem. 275*, 37181–37186.
45. Jamin, N., Neumann, J. M., Ostuni, M. A., Vu, T. K., Yao, Z. X., Murail, S., Robert, J. C., Giatzakis, C., Papadopoulos, V., and Lacapere, J. J. (2005) Characterization of the cholesterol recognition amino acid consensus sequence of the peripheral-type benzodiazepine receptor. *Mol. Endocrinol. 19*, 588–594.
46. Viguera, A. R., and Serrano, L. (1995) Experimental analysis of the Schellman motif. *J. Mol. Biol. 251*, 150–160.
47. Li, W., Amri, H., Huang, H., Wu, C., and Papadopoulos, V. (2004) Gene and protein profiling of the response of MA-10 Leydig

tumor cells to human chorionic gonadotropin. *J. Androl. 25*, 900–913.
48. Walther, D. M., and Rapaport, D. (2009) Biogenesis of mitochondrial outer membrane proteins. *Biochim. Biophys. Acta 1793*, 42–51.
49. Rone, M. B., Fan, J., and Papadopoulos, V. (2009) Cholesterol transport in steroid biosynthesis: Role of protein-protein interactions and implications in disease states. *Biochim. Biophys. Acta 1791*, 646–658.
50. Thomson, M. (1998) Molecular and cellular mechanisms used in the acute phase of stimulated steroidogenesis. *Horm. Metab. Res. 30*, 16–28.
51. Brdiczka, D. G., Zorov, D. B., and Sheu, S. S. (2006) Mitochondrial contact sites: Their role in energy metabolism and apoptosis. *Biochim. Biophys. Acta 1762*, 148–163.
52. Reichert, A. S., and Neupert, W. (2002) Contact sites between the outer and inner membrane of mitochondria-role in protein transport. *Biochim. Biophys. Acta 1592*, 41–49.